American Physical Society
1963 Summer Meeting in the West
Edmonton, CANADA
August 28-30, 1963

Elastic Scattering of He^3 at 20 Mev+

Raymond W. Klingensmith*
Battelle Memorial Institute, Columbus, Ohio

and

Hershel J. Hausman and William D. Ploughe
The Ohio State University, Columbus, Ohio

Van de Graaff Accelerator Laboratory

THE OHIO STATE UNIVERSITY
DEPARTMENT OF PHYSICS
COLUMBUS, OHIO

Elastic Scattering of He^3 at 20 Mev+

Raymond W. Klingensmith*
Battelle Memorial Institute, Columbus, Ohio

and

Hershel J. Hausman and William D. Ploughe
The Ohio State University, Columbus, Ohio

Note added in proof:

Error flags were inadvertently left off of the figures.

Table I presents the data as obtained from the computer outputs. The number of significant figures by no means reflects the accuracy of the data.

Elastic Scattering of He^3 at 20 Mev[+]

Raymond W. Klingensmith*
Battelle Memorial Institute, Columbus, Ohio

and

Hershel J. Hausman and William D. Ploughe
The Ohio State University, Columbus, Ohio

ABSTRACT

Absolute differential elastic scattering cross sections were measured for the scattering of 20 Mev He^3 particles from V, Ni, Cu, Rh, Sn^{118}, Sm, Yb, and Pb. Where practical the measurements were made at laboratory angles extending from 20 degrees to 170 degrees. The diffraction-like oscillations exhibited by the elastic-to-Coulomb cross section ratios are not highly pronounced. A preliminary optical model analysis was carried out using the HUNTER automatic search code of Drisko and Bassel. A Woods-Saxon potential with Thomas type spin-orbit coupling was considered. Reasonable fits to the data were obtained.

INTRODUCTION

Absolute differential elastic scattering cross sections were measured at 20 Mev for V, Ni, Cu, Rh, Sn^{118}, Sm, Yb, and Pb from 20 degrees to 170 degrees (laboratory angles). The measurements were made to provide He^3 data at this energy over a wide range of the periodic table. It is expected that these data will complement those at both higher and lower energies.[1,2,3] As expected, the elastic-to-Coulomb cross section ratio was found to deviate from unity but the diffraction-like oscillations are not highly pronounced. In addition to the listed elements, measurements were carried out for yttrium and bismuth. However, due to experimental difficulties these data have not yet been analyzed. A preliminary optical model analysis of the data was carried out. The intent of the analysis is to indicate the general applicability of the model to the data and to obtain reasonable model parameters.

EXPERIMENTAL APPARATUS AND TECHNIQUES

Doubly ionized He^3 ions were accelerated to an energy of 20.0 ± 0.2 Mev in The Ohio State University cyclotron. The beam was extracted from the cyclotron chamber and focused by a pair of quadrupole magnets and a 15 degree beam-analyzing magnet onto a target located at the center of a 22 inch diameter scattering chamber. Within the scattering chamber, a rotating platform, driven by a remotely controlled variable-speed dc motor, carried the scattered-particle detector and collimator through an angular span of 170 degrees (laboratory). The angular position of the detector was tracked by a pair of Selsyn motors and measured to an absolute accuracy of ± 0.1 degree.

A movable target holder capable of supporting three mounted targets was located at the center of the scattering chamber. The holder could be moved vertically and rotated about its vertical axis without breaking the chamber vacuum. An external scale indicated the position of the holder with respect to each mode of movement. Positioning of the holder was done manually and was independent of all other movements within the chamber.

The beam collimator consisted of a tapered brass tube 8.1 inches long with aluminum defining apertures press fitted into the ends. The final aperture was 0.064 inch in diameter and was located three inches from the center of the chamber. In addition, a slightly larger aperture at the center of the tube reduced internal beam scatter. The resulting beam spot, as it appears at the target, was a well defined circle with a diameter of approximately 0.1 inch.

The targets consisted of thin foils mounted in brass frames designed to fit into the holder in the scattering chamber. The several targets varied in thickness from 0.332 mg/cm^2 to 8.27 mg/cm^2. Thickness measurements were considered accurate only to $\pm$ 10 per cent. The lead target was mounted on a 0.02 mg/cm^2 aluminum backing. All other targets were self-supporting.

A gold-silicon surface barrier solid-state detector was used as the scattered-particle detector. The resolution of the detector was measured and found to be 37 Kev, FWHM for 5.30 Mev alpha particles. A dc bias voltage of 120 volts applied to the detector created a depletion region 340 microns in depth. This depth was sufficient to stop 25 Mev He^3 particles and proved

adequate for this experiment. A solid angle of 3.42×10^{-4} steradians was subtended at the detector by means of a collimator. Measurements of this solid angle over the range zero degrees to 170 degrees (laboratory) indicated its value to be constant to within one per cent.

A closed-loop gas handling system was provided in order to reduce to a minimum the inventory of He^3 gas necessary. The system was patterned after the Los Alamos system[4] and consisted essentially of a main recirculating loop and a series of smaller loops which transferred the gas to a storage tank. Only minor modification of the pumps was necessary to provide adequate integrity for the He^3 application. When the cyclotron was not in use or when other ions were being accelerated, the He^3 gas was pumped out of the recirculating loop and into the storage tank.

ANALYSIS OF THE EXPERIMENTAL DATA

An optical model analysis of the experimental data was made using the HUNTER computer code of Drisko and Bassel.[5] The HUNTER code combines an optical model calculation of differential elastic scattering cross sections and the associated elastic-to-Coulomb ratios with an automatic search of the optical potential parameters. Gross agreement between the calculated cross sections and the corresponding experimental data is indicated by a Chi-square (χ^2) test.

The analysis carried out in this experiment considered an optical potential of the Woods-Saxon form with a Thomas type spin-orbit interaction:

$$V_I = (V_o + iW_o)\left[1 + e^{\frac{r-R}{a}}\right]^{-1} + \left[\frac{\hbar}{M_\pi C}\right]^2 V_s \vec{\sigma}\cdot\vec{L}\,\frac{1}{r}\frac{d}{dr}\left[1 + e^{\frac{r-R}{a}}\right]^{-1} + V_c \qquad 5$$

The calculations for this analysis were done at Oak Ridge, Tennessee on the Union Carbide Central Data Processing Facility IBM-7090 digital computer. The initial set of parameters chosen was that obtained by Bassel[6] from an analysis of the 30 Mev He^3 elastic scattering data of Greenlees et al.[1,2] The parameters represent the average optimum set for V, Ni, and Cu and will henceforth be referred to as the average 30 Mev parameters.

The calculations were relatively insensitive to the values of V_s and R_c. Therefore, in all but a few special cases, V_s was held fixed at 8 Mev and R_c was held fixed at 1.3 fermis for V, Ni, Cu, Rh, Sn^{118}, and Sm, 1.4 fermis for Yb, and 1.5 fermis for Pb. In all cases a maximum of twenty partial waves was sufficient.

After the first few searches had been made, it was found that the experimental points for nickel, copper, and lead all were significantly displaced from the calculated curves, indicating an error in the absolute normalization of the measured cross sections. A similar but smaller displacement was noted in the tin-118, samarium, and ytterbium data. Included in the HUNTER program is the calculation of a multiplicative factor to correct for this displacement. By multiplying the measured cross sections by the calculated displacement-correction factor, the value of χ^2 is minimized without affecting the shape of the distribution.

Table I contains the measured cross sections as a function of center-of-mass scattering angle. The relative error associated with the measured

cross-sections is estimated to be less than ten percent. The angular distributions of the elastic-to-Coulomb cross-section ratio, as obtained from the displacement-corrected cross sections, are also included in Table I.

During the analysis many searches were conducted. As a result several sets of parameters were obtained for each element. In many cases the value of χ^2 was relatively small though not absolutely minimized. Following the suggestion of Bjorklund et al.[7] that the real part of the nuclear potential is a function of Z_1, Z_2 and mass number, A, through the relation

$$V_o = K_1 + K_2 Z_1 Z_2 A^{-1/3}$$

the various values of V_o were plotted against $Z_1 Z_2 A^{-1/3}$.

The nuclear radius is defined for the Woods-Saxon form factor as

$$R = R_o A^{1/3}.$$

Several studies[8,9,10] have indicated that good fits to experimental data can be obtained if the nuclear radius is defined as

$$R = C_1 A^{1/3} + C_2 = (C_1 + C_2 A^{-1/3}) A^{1/3}$$

This suggests that the nuclear radius parameter depends upon A through the relation

$$R_o = C_1 + C_2 A^{-1/3}$$

Consequently, R_o was plotted against $A^{-1/3}$.

Values of the diffusivity parameter a, showed a tendency to decrease with increasing mass number. This effect can be loosely attributed to the increasing Coulomb barrier resulting in a lower effective incident particle energy. As a

result the target nucleus shows a greater reflection coefficient by means of a smaller diffusivity parameter. To illustrate this decreasing tendency, a was plotted against the target mass number, A.

By correlating the best curves through the spread of data it was possible to establish two distinct trends:

Trend A $V_o = 33 + 1.75\ Z_1 Z_2\ A^{-1/3}$

$R_o = 1.27 + 1.25\ A^{-1/3}$

$a = 0.658 - .0008\ A$

Trend B $V_o = 27 + 1.97\ Z_1 Z_2\ A^{-1/3}$

$R_o = 1.47 + 0.2\ A^{-1/3}$

$a = 0.658 - .0008\ A$

No correlation could be found for the imaginary part of the nuclear potential, W_o. The only difference between the two trends is in the vanadium, rhodium, and tin parameters.

The optimum parameters associated with each trend are listed in Table II. The plots of V_o against $Z_1 Z_2\ A^{-1/3}$, R_o against $A^{-1/3}$, and a against A are given in Figures 1 and 2.

The establishment by Bassel of an average set of parameters for 30 Mev He^3 elastic scattering from vanadium, nickel, and copper suggests that average parameters for these elements may exist for 20 Mev scattering. The best parameters obtained in the present analysis for vanadium and copper do not

differ greatly and were therefore averaged to give a single set. These parameters are referred to as the average 20 Mev parameters. Table III lists the average 20 Mev parameters obtained in this analysis and the average 30 Mev parameters of Bassel. Good fits to the vanadium and copper data are obtained using the average 20 Mev parameters. However, the experimental data extend only to 110 degrees. The nickel data, which extend to 170 degrees, are fit equally well up to 110 degrees, but very poorly beyond; the theoretical curve oscillating too vigorously. Using the experimental data obtained for vanadium and copper precluded HUNTER calculations of the back angle curve. This is because the code is programmed to provide calculations only at angles for which input cross sections are given. In order to obtain an indication of the degree of oscillation in the vanadium and copper angular distribution curves at back angles, HUNTER calculations were forced to 170 degrees by providing as input, extrapolations of the experimental data. This was done for only one case and used the average 20 Mev parameters. The resulting curves showed oscillations similar to those of the nickel curve.

Figures 3 and 4 contain the theoretical angular distribution curves as obtained from the optimum parameters and the displacement-corrected cross sections. The shapes of the vanadium and copper curves beyond 110 degrees as obtained from the forced HUNTER calculations are indicated.

COMPARISON WITH OTHER RESULTS

The average 20 Mev parameters established in the experiment for vanadium, nickel and copper can be compared to the average 30 Mev parameters established for vanadium, nickel, and copper by Bassel. The real part of the nuclear potential is larger in the 30 Mev case while the radius parameter is smaller. The other parameters are relatively unchanged. However, it must be noted that these parameters are based on experimental data extending to scattering angles no greater than 120 degrees.

Extensive optical model analyses of 30 Mev He^3 scattering data have been done by Hodgson et al.[11, 12, 13] and Greenlees et al.[2] These analyses tend to equalize the values of the real and imaginary parts of the nuclear potential at approximately 30-50 Mev. In the analysis conducted for the present experiment, the imaginary part of the potential was held to a value less than that of the real part; the ratio being approximately two or three to one. Consequently, quantitative comparison with the Hodgson results cannot be readily made.

CONCLUSIONS

Departures from Coulomb scattering have been observed in the elastic scattering of 20 Mev He^3 particles from V, Ni, Cu, Rh, Sn^{118}, Sm, Yb, and Pb. Diffraction-like oscillations in the elastic-to-Coulomb cross section ratio are evident, although not pronounced, in the lighter element data.

The optical model analysis carried out in the experiment considered only a Woods-Saxon type potential with a Thomas type spin-orbit interaction. In this regard the analysis cannot be considered exhaustive even though reasonable fits to the data are obtained and trends among the parameters noted.

Experimental data for vanadium and copper were obtained at scattering angles extending only to 110 degrees. An average set of parameters was established which gives good fits to these data. The same set of parameters gives a good fit to the nickel data up to 110 degrees, but gives an angular distribution for the cross section which oscillates too vigorously beyond 110 degrees. By providing extrapolated input data to the HUNTER program, calculations of the back angle cross sections for vanadium and copper using the average 20 Mev parameters were obtained. Oscillations similar to those for nickel were indicated.

The relatively small oscillations in the observed nickel cross sections suggest that only small oscillations may exist in the vanadium and copper cross sections. Consequently, the average 20 Mev parameters established in this experiment and the average 30 Mev parameters established by Bassel may not provide a good fit to the data at back angles. In this regard, an interesting extension of both the present experiment and the 30 Mev experiment would be the investigation of back angle elastic scattering for elements below copper.

The results obtained for the heavy elements show a smooth and gradual departure from Coulomb scattering at large angles. As a result, equally good fits to the data are obtained with a wide choice of parameters. In order to unambiguously define the parameters, additional data are needed. Analysis of reaction cross sections provides a means of determining the nuclear absorption, and hence, leads to values for W_o as well as defining the form factors. In addition, polarization studies are needed to establish the form of the spin-orbit potential.

ACKNOWLEDGMENTS

The authors wish to acknowledge the excellent and continued assistance provided by the staffs of The Ohio State University Cyclotron Laboratory and Electrostatic Generator Laboratory. One of us (R. W. K.) is indebted to Battelle Memorial Institute for the Battelle Staff Fellowship given in support of this research.

In addition we are indebted to Dr. R. H. Bassel of the Oak Ridge National Laboratory for his continued interest in this work and his guidance in the analysis of the experiment. Particular acknowledgement is given Dr. Bassel for providing both the results of his 30 MeV analysis and use of the HUNTER program prior to publication.

Gratitude is expressed to the Oak Ridge National Laboratory for the hospitality and cooperation extended in the use of the computer and other analytical facilities.

REFERENCES

[†]This work was supported in part by the National Science Foundation.

[*]This article is based on a portion of a doctoral thesis submitted by R. W. Klingensmith to the faculty of The Ohio State University.

[1]G. W. Greenlees and R. C. Rowe, Nuclear Phys. 15, 687 (1960).

[2]G. W. Greenlees, J. S. Lilley, and R. C. Rowe, Nuclear Phys. 24, 334 (1961).

[3]H. E. Wegner, Los Alamos Scientific Laboratory, Los Alamos, New Mexico (to be published).

[4]H. E. Wegner and W. S. Hall, Rev. Sci. Instr. 29, 1100 (1958).

[5]R. Drisko and R. H. Bassel, Oak Ridge National Laboratory, Oak Ridge, Tennessee (Unpublished).

[6]R. H. Bassel, Oak Ridge National Laboratory, Oak Ridge, Tennessee (Private Communication).

[7]F. E. Bjorklund, G. Campbell, and S. Fernbach, Proc. Int. Symposium on Polarization Phenomena of Nucleons (Basel, 1961).

[8]M. A. Melkanoff, J. S. Nodvick, D. S. Saxon, and R. O. Woods, Phys. Rev. 106, 1319 (1957).

[9]J. R. Beyster, M. Walt, and E. W. Salmi, Phys. Rev. 106, 1319 (1957).

[10]G. Igo and R. M. Thaler, Phys. Rev. 106, 126 (1957).

[11]P. E. Hodgson, Nuclear Phys. 21, 28 (1960).

[12]P. E. Hodgson, Nuclear Phys. 23, 499 (1961).

[13]J. Aguilar, A. Garcia, J. B. S. England, P. E. Hodgson, and W. T. Toner, Nuclear Phys. 25, 259 (1961).

TABLE I

Absolute elastic cross sections and elastic-to-Coulomb cross section ratios vs. center-of-mass scattering angle for 20 Mev He^3 scattered from several elements.

Vanadium (B = 1.00)*			Nickel (B = 1.19)		
Θ_{CM} (degrees)	$(\sigma_E)_{CM}$ (mb/str)	$(\sigma_E/\sigma_R)_{CM}$	Θ_{CM} (degrees)	$(\sigma_E)_{CM}$ (mb/str)	$(\sigma_E/\sigma_R)_{CM}$
21.24	6381	.869	21.09	7987	.9351
26.51	1872	.611	26.32	2571	.7200
26.51	1835	.599	31.55	1064	.6060
26.51	1799	.587	36.77	459.9	.4742
31.78	785.2	.520	41.97	199.8	.3424
37.03	331.5	.397	47.16	104.5	.2787
42.26	140.8	.280	52.33	57.53	.2267
42.26	151.9	.303	57.49	31.80	.1773
42.26	150.7	.300	62.63	20.62	.1568
42.26	149.4	.298	67.75	13.36	.1344
42.26	148.2	.295	72.84	7.887	.1021
44.87	100.7	.252	77.92	4.850	.0790
44.87	102.1	.255	82.98	3.693	.0741
47.48	75.51	.234	88.01	2.400	.0582
47.48	76.75	.238	88.01	2.708	.0653
52.68	44.11	.201	93.02	1.744	.0503
57.86	24.76	.160	98.01	1.192	.0403
63.02	14.65	.129	102.97	.844	.0321
65.59	11.23	.114	102.97	.835	.0321
65.59	11.52	.117	102.97	.880	.0333
68.15	8.821	.102	107.92	.677	.0301
68.15	9.220	.107	112.84	.507	.0241
73.27	5.322	.079	112.84	.513	.0249
73.27	5.335	.079	112.84	.497	.0238
78.36	3.329	.062	117.74	.395	.0221
78.36	3.290	.061	122.62	.310	.0190
80.89	2.740	.057	122.62	.291	.0178
83.42	2.251	.052	127.48	.261	.0176
83.42	2.436	.056	132.33	.225	.0164
83.42	2.357	.054	141.96	.152	.0127
88.46	1.832	.051	151.54	.118	.0108
88.46	1.859	.051	161.08	.110	.0109
93.47	1.324	.043			
93.47	1.221	.040			
98.46	.844	.032			
98.46	.8249	.032			
103.42	.4815	.021			
103.42	.4636	.020			

* B = Displacement correction factor by which measured cross sections are multiplied to agree with theoretical distribution.

TABLE I (continued) --2

Copper (B = 1.24)			Rhodium (B = 1.00)		
Θ_{CM} (degrees)	$(\sigma_E)_{CM}$ (mb/str)	$(\sigma_E/\sigma_R)_{CM}$	Θ_{CM} (degrees)	$(\sigma_E)_{CM}$ (mb/str)	$(\sigma_E/\sigma_R)_{CM}$
21.01	9066	1.014	20.65	27010	.992
26.23	3045	.8160	25.79	11320	.999
26.23	3094	.8281	30.92	5939	1.070
26.23	3072	.8279	36.04	3057	.996
31.44	1226	.6681	41.16	1703	.925
31.44	1236	.6750	46.26	941.2	.799
36.64	558.8	.5520	48.82	733.2	.759
36.64	553.3	.5455	48.82	726.0	.752
36.64	540.3	.5341	51.36	528.0	.663
41.83	254.6	.4180	56.45	311.9	.555
41.83	251.3	.4131	61.53	190.1	.462
41.83	248.6	.4075	61.53	188.3	.458
47.00	132.6	.3392	64.07	135.9	.382
52.16	72.25	.2731	64.07	146.1	.410
57.31	40.58	.2172	66.60	121.5	.392
62.43	22.63	.1652	66.60	119.1	.384
67.54	14.35	.1387	71.65	76.22	.317
72.63	8.680	.1081	76.70	50.51	.265
77.70	5.432	.0831	79.22	36.64	.215
77.70	5.415	.0843	81.73	35.25	.229
77.70	5.335	.0841	86.75	20.77	.164
82.76	3.620	.0694	91.75	18.12	.171
82.76	3.383	.0645	96.75	13.64	.151
87.79	2.551	.0597	101.73	10.77	.138
92.80	1.705	.0471	111.65	5.708	.095
92.80	1.664	.0459	121.53	3.341	.068
97.79	1.146	.0374	131.36	2.111	.051
102.75	.834	.0314	141.15	1.242	.034
107.70	.559	.0241	150.91	.9184	.028
112.63	.424	.0206	150.91	1.051	.032
122.43	.268	.0160			

TABLE I (continued--3)

Tin-118 (B = 1.07)			Samarium (B = 0.95)		
Θ_{CM} (degrees)	$(\sigma_E)_{CM}$ (mb/str)	$(\sigma_E/\sigma_R)_{CM}$	Θ_{CM} (degrees)	$(\sigma_E)_{CM}$ (mb/str)	$(\sigma_E/\sigma_R)_{CM}$
15.46	100500	1.010	20.47	56860	1.011
20.58	31700	.991	25.56	22730	.971
25.70	13530	1.018	30.65	10760	.936
25.70	13180	.990	35.74	5992	.948
25.70	13710	1.030	40.82	3691	.974
30.81	6586	1.008	40.82	3601	.948
30.81	6932	1.060	45.89	2427	1.000
30.81	6622	1.012	50.96	1601	.978
35.92	3740	1.038	56.02	1152	.999
41.02	2316	1.070	61.07	801.6	.953
41.02	2209	1.022	66.12	582.3	.920
46.11	1394	1.006	71.16	412.9	.844
51.20	821.2	.879	76.19	303.1	.783
56.28	494.8	.750	81.21	223.0	.647
56.28	490.3	.744	86.22	163.7	.636
61.35	310.6	.646	91.22	122.5	.570
66.40	198.5	.548	96.22	92.78	.507
71.45	135.6	.484	96.22	95.94	.524
76.49	86.03	.388	101.21	74.12	.471
81.52	57.94	.323	101.21	70.57	.448
86.54	39.38	.267	106.19	59.00	.430
91.54	30.20	.251	111.15	46.21	.381
96.53	22.14	.211	111.15	44.61	.368
101.52	16.63	.183	116.12	38.71	.358
101.52	16.82	.185	121.07	28.88	.296
101.52	16.26	.179	121.07	28.60	.293
106.49	12.29	.155	126.02	23.84	.267
111.45	9.711	.136	126.02	24.79	.276
111.45	9.522	.138	130.95	21.30	.236
116.40	7.877	.126	135.89	18.71	.246
121.34	6.368	.113	135.89	17.19	.225
121.34	5.769	.102	140.81	17.23	.241
126.27	4.627	.0890	140.81	13.97	.196
131.20	3.887	.0814	145.73	14.00	.208
131.20	3.801	.0794	145.73	14.29	.212
136.11	3.083	.0700	150.65	12.49	.195
141.02	2.688	.0651	155.56	11.74	.191
145.91	2.338	.0600	160.47	10.70	.180
150.81	1.985	.0525	165.37	10.61	.183
150.81	2.053	.0546	170.27	10.33	.182
155.69	1.805	.0506			
160.57	1.682	.0481			
160.57	1.672	.0480			
165.45	1.596	.0474			
169.35	1.568	.0473			

TABLE I (Continued--4)

Ytterbium (B = 0.98)			Lead (B = 1.28)		
Θ_{CM} (degrees)	$(\sigma_E)_{CM}$ (mb/str)	$(\sigma_E/\sigma_R)_{CM}$	Θ_{CM} (degrees)	$(\sigma_E)_{CM}$ (mb/str)	$(\sigma_E/\sigma_R)_{CM}$
20.42	68710	.999	20.36	71830	.999
25.50	29400	1.008	25.43	30150	.979
30.58	14300	1.010	30.49	14850	1.012
35.65	7870	1.018	35.55	8100	1.005
40.72	4993	1.098	40.61	4858	1.004
40.72	4836	1.041	45.67	3132	1.012
45.78	2976	1.003	50.71	2101	1.006
50.84	2027	1.013	55.76	1470	1.002
55.89	1428	.975	60.80	1087	1.015
60.94	1069	1.040	65.83	795.6	.988
60.94	1061	1.035	70.86	626.3	1.010
65.98	787.3	1.018	70.86	630.4	1.015
65.98	819.2	1.062	75.88	501.1	1.020
71.01	600.1	1.008	80.90	408.2	1.030
71.01	592.1	.995	85.91	329.8	1.013
76.04	444.0	.942	90.91	274.4	1.009
76.04	468.1	1.008	95.91	238.3	.989
81.06	351.4	.924	100.90	202.7	1.022
81.06	338.0	.885	100.90	191.7	.966
86.07	264.5	.845	105.88	165.9	.959
86.07	269.1	.860	110.86	142.7	.935
91.07	214.8	.821	115.83	125.0	.918
96.07	164.0	.739	120.80	108.3	.882
96.07	170.8	.770	125.76	95.72	.856
101.06	130.6	.684	130.71	87.66	.852
101.06	134.4	.704	135.66	79.28	.831
106.04	110.8	.666	140.61	72.82	.815
106.04	108.9	.654	145.55	67.46	.800
111.01	87.68	.596	150.49	61.36	.764
111.01	92.60	.629	155.43	57.48	.746
115.98	74.51	.568	160.36	55.71	.748
115.98	75.33	.571	165.29	52.93	.730
115.98	75.06	.569	170.22	50.98	.716
115.98	72.04	.549			
120.94	65.92	.556			
125.89	54.52	.505			
130.84	47.48	.478			
135.78	40.39	.438			
140.72	34.93	.405			
145.65	31.94	.392			
150.57	29.49	.380			
155.50	27.86	.374			
160.42	26.69	.371			
165.33	24.26	.346			
170.25	23.88	.347			

TABLE II

OPTIMUM PARAMETERS FOR TRENDS A AND B

		V_o (Mev)	W_o (Mev)	R_o (fm)	a (fm)	R_c (fm)	V_s (Mev)	χ^2
A	V	54.8	11.87	1.477	.618	1.3	8	46.1
	Ni	60.1	23.5	1.597	.600	1.3	8	41
	Cu	55.2	16.4	1.475	.628	1.3	8	31
	Rh	67.8	14.2	1.54	.55	1.3	8	70.3
	Sn	68.5	14.4	1.52	.55	1.3	8	27.9
	Sm	74.4	47.6	1.51	.55	1.3	8	32
	Yb	77.1	10.0	1.50	.51	1.4	8	41.1
	Pb	80.5	1.73	1.50	.51	1.5	8	4.1
B	V	51.6	13.4	1.52	.619	1.3	8	59.8
	Ni	60.1	23.5	1.597	.600	1.3	8	41
	Cu	55.2	16.4	1.475	.628	1.3	8	31
	Rh	63.1	27.7	1.50	.60	1.3	8	62.6
	Sn	67.6	13.8	1.51	.551	1.3	8	27.9
	Sm	74.4	47.6	1.51	.55	1.3	8	32
	Yb	77.1	10.0	1.50	.51	1.4	8	41.1
	Pb	80.5	1.73	1.50	.51	1.5	8	4.1

TABLE III

AVERAGE OPTICAL MODEL PARAMETERS FOR VANADIUM, NICKEL AND COPPER AT 20 AND 30 MEV

	20 Mev	30 Mev[a]
V_o (Mev)	55.0	68.1
W_o (Mev)	14.6	14.4
a (fermis)	0.62	0.611
R_o (fermis)	1.475	1.508
R_c (fermis)	1.3	1.3
V_s (Mev)	8	8

[a]See reference 6.

FIGURE CAPTIONS

FIGURE 1. Plots of mass number (A) vs diffusivity parameter (a), nuclear radius parameter (R_o) vs. $A^{-1/3}$, depth of the real part of the optical potential ($V_o + i\ W_o$) vs. $Z_1 Z_2\ A^{-1/3}$ for the elastic scattering of 20 Mev He^3. The optical model parameters are those of Trend A given in Table I.

FIGURE 2. Plots of mass number (A) vs diffusivity parameter (a), nuclear radius parameter (R_o) vs. $A^{-1/3}$, depth of the real part of the optical potential ($V_o + i\ W_o$) vs. $Z_1 Z_2\ A^{-1/3}$ for the elastic scattering of 20 Mev He^3. The optical model parameters are those of Trend B given in Table I.

FIGURE 3. Angular distributions of the elastic-to-Coulomb cross section ratio for the scattering of He^3 by (a) vanadium, (b) nickel, (c) copper, (d) rhodium. The smooth curves represent the distributions given by the optimum parameters as determined using the HUNTER search code.

FIGURE 4. Angular distributions of the elastic-to-Coulomb cross section ratio for the scattering of He^3 by (a) tin-118, (b) samarium, (c) ytterbium, (d) lead. The smooth curves represent the distributions given by the optimum parameters as determined using the HUNTER search code.

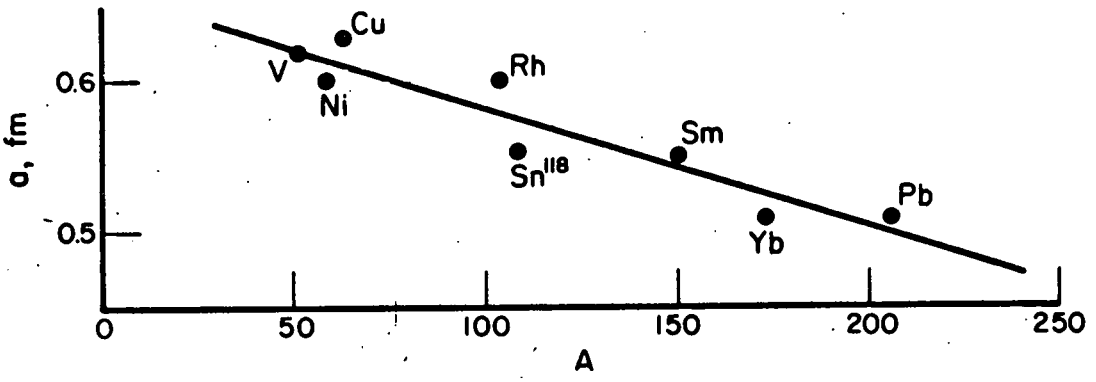
a, fm
0.6
0.5
Cu
V
Ni
Rh
Sn118
Sm
Yb
Pb
0
50
100
150
200
250
A

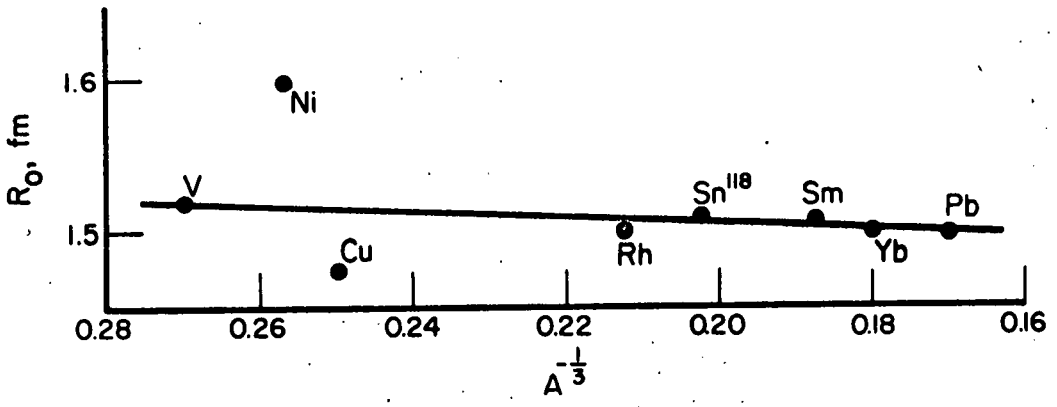
R0, fm
1.6
1.5
Ni
V
Cu
Rh
Sn118
Sm
Yb
Pb
0.28
0.26
0.24
0.22
0.20
0.18
0.16
A-1/3

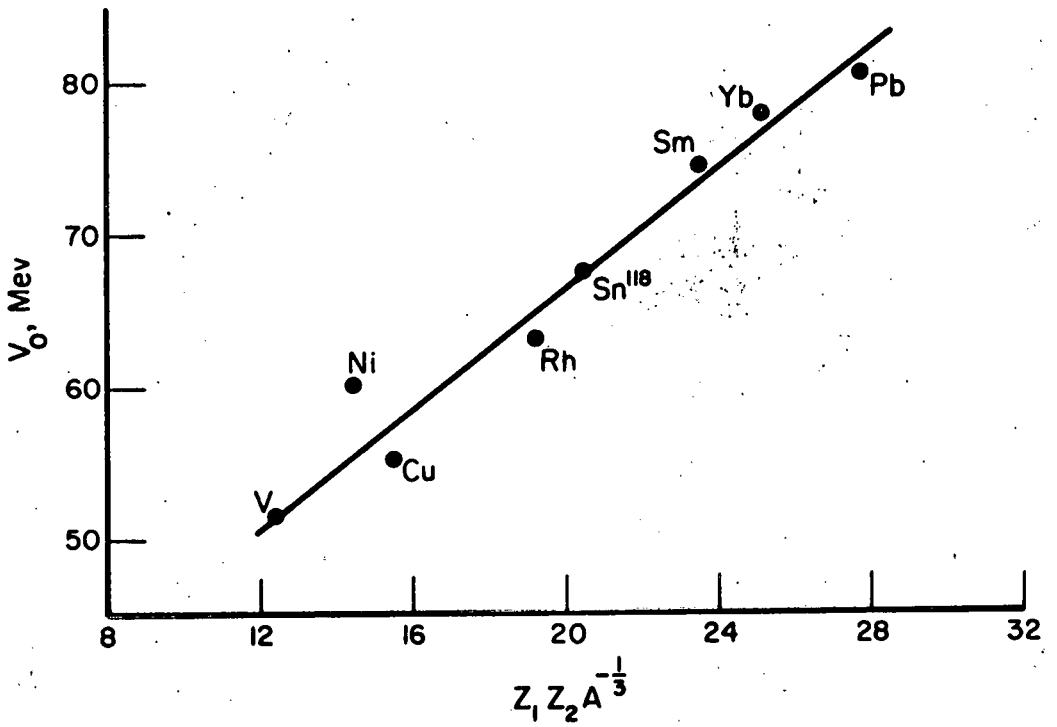
V0, Mev
80
70
60
50
Yb
Pb
Sm
Sn118
Ni
Rh
Cu
V
8
12
16
20
24
28
32
Z1 Z2 A-1/3

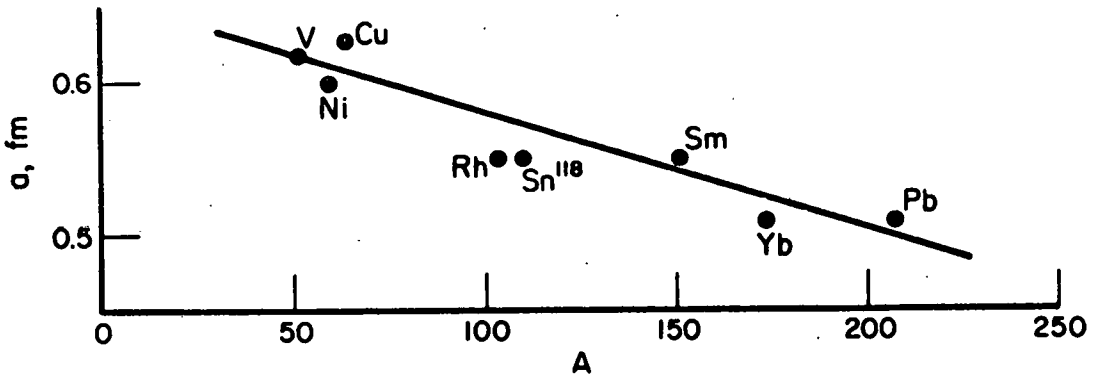
a, fm
0.6
0.5
V
Cu
Ni
Rh
Sn118
Sm
Yb
Pb
0
50
100
150
200
250
A

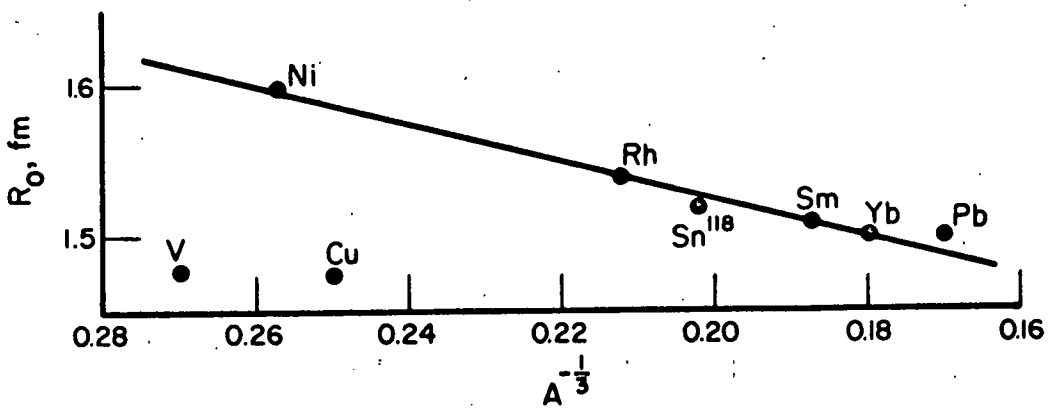
R0, fm
1.6
1.5
Ni
Rh
Sn118
Sm
Yb
Pb
V
Cu
0.28
0.26
0.24
0.22
0.20
0.18
0.16
A-1/3

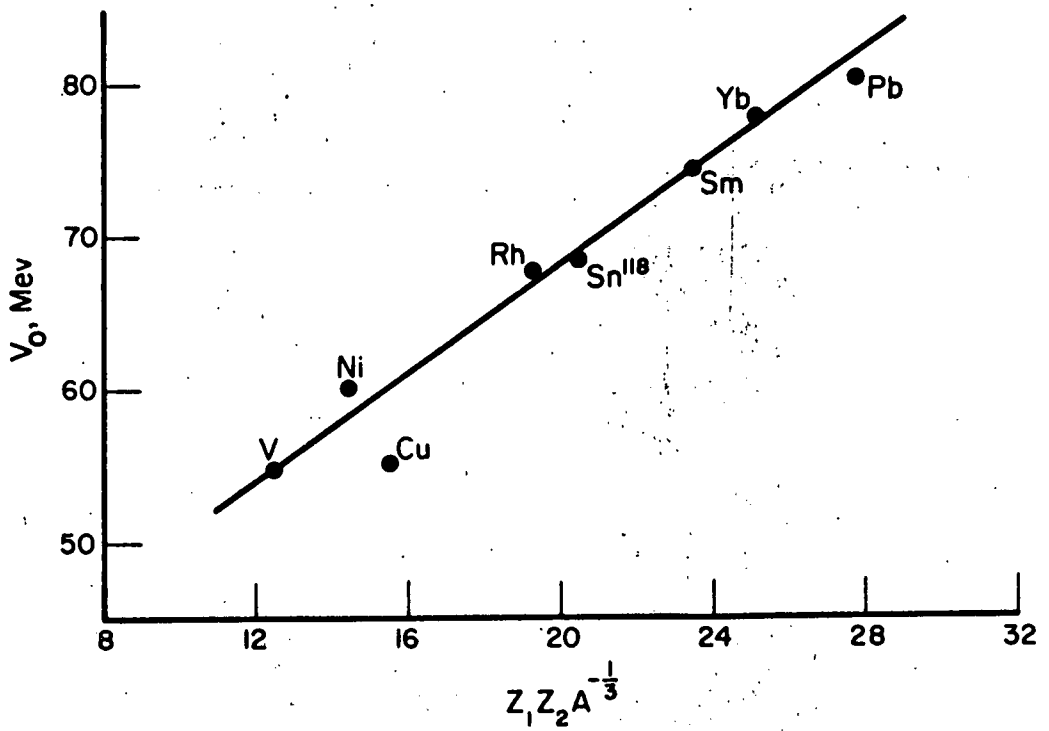
V0, Mev
80
70
60
50
Yb
Pb
Sm
Rh
Sn118
Ni
V
Cu
8
12
16
20
24
28
32
Z1Z2A-1/3

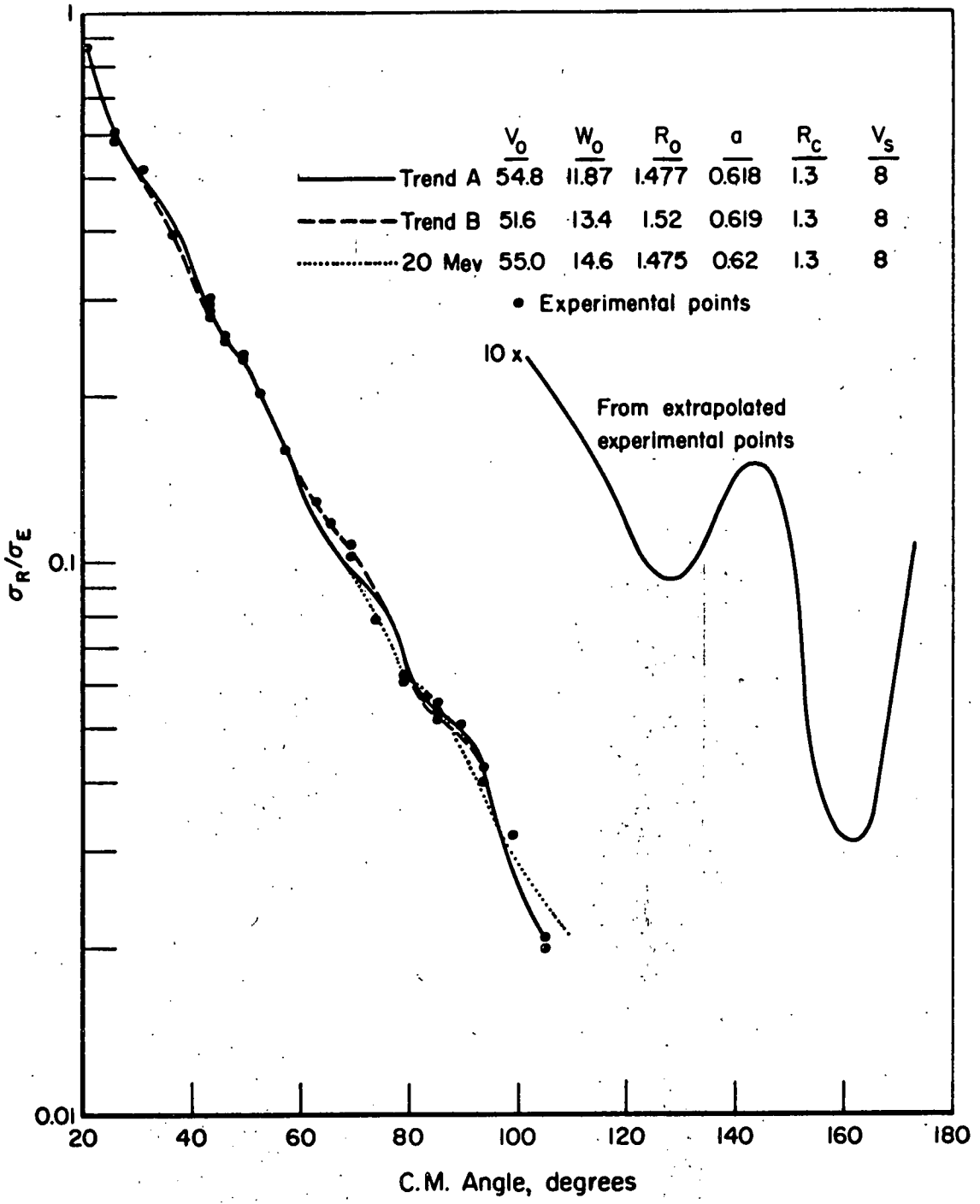
V_0 W_0 R_0 a R_c V_s
Trend A 54.8 11.87 1.477 0.618 1.3 8
Trend B 51.6 13.4 1.52 0.619 1.3 8
20 Mev 55.0 14.6 1.475 0.62 1.3 8
• Experimental points
10 x
From extrapolated experimental points
σ_R/σ_E
1
0.1
0.01
20
40
60
80
100
120
140
160
180
C.M. Angle, degrees

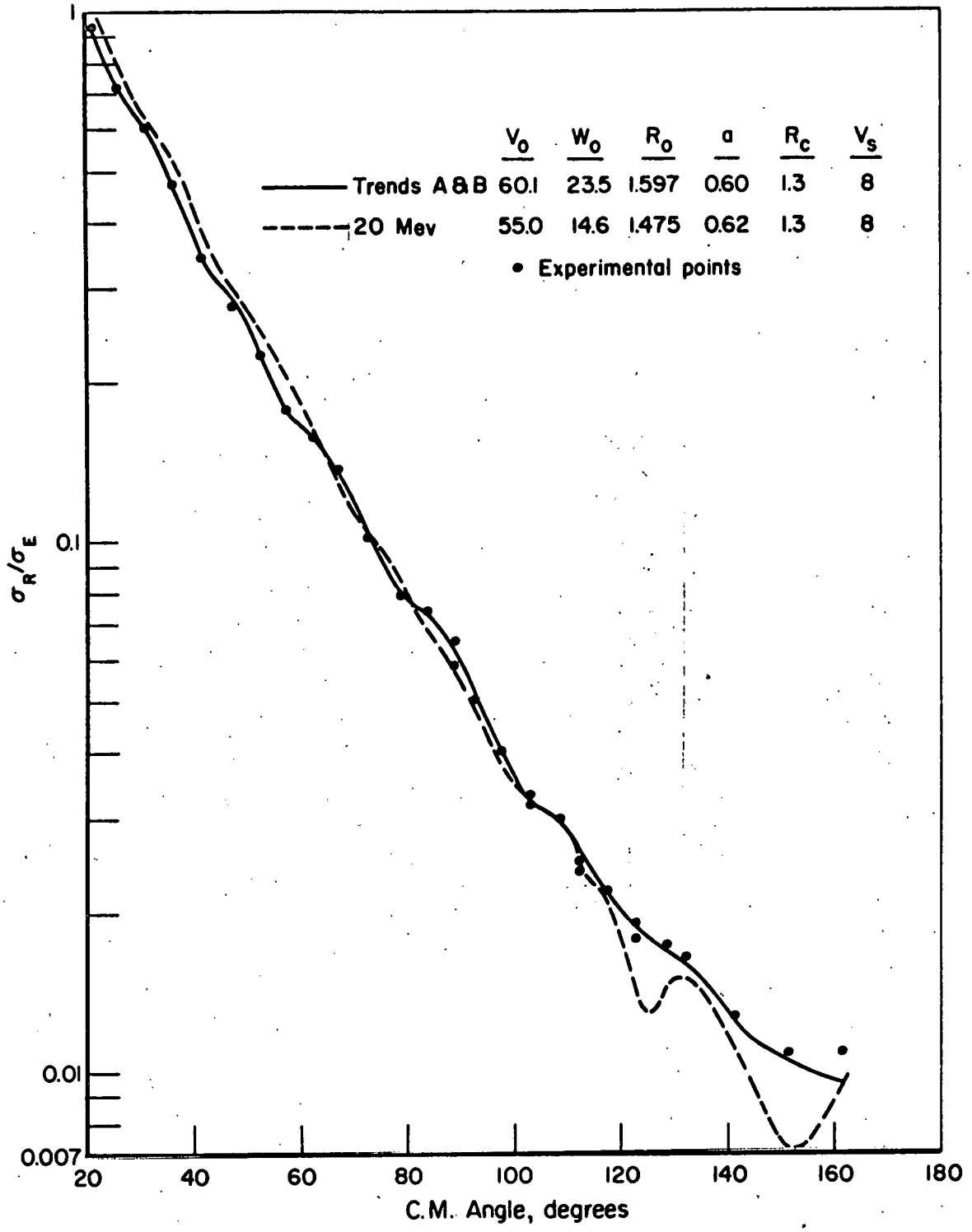
1
0.1
0.01
0.007
σ_R/σ_E
20
40
60
80
100
120
140
160
180
C.M. Angle, degrees
V_0 W_0 R_0 a R_C V_s
Trends A&B 60.1 23.5 1.597 0.60 1.3 8
20 Mev 55.0 14.6 1.475 0.62 1.3 8
• Experimental points

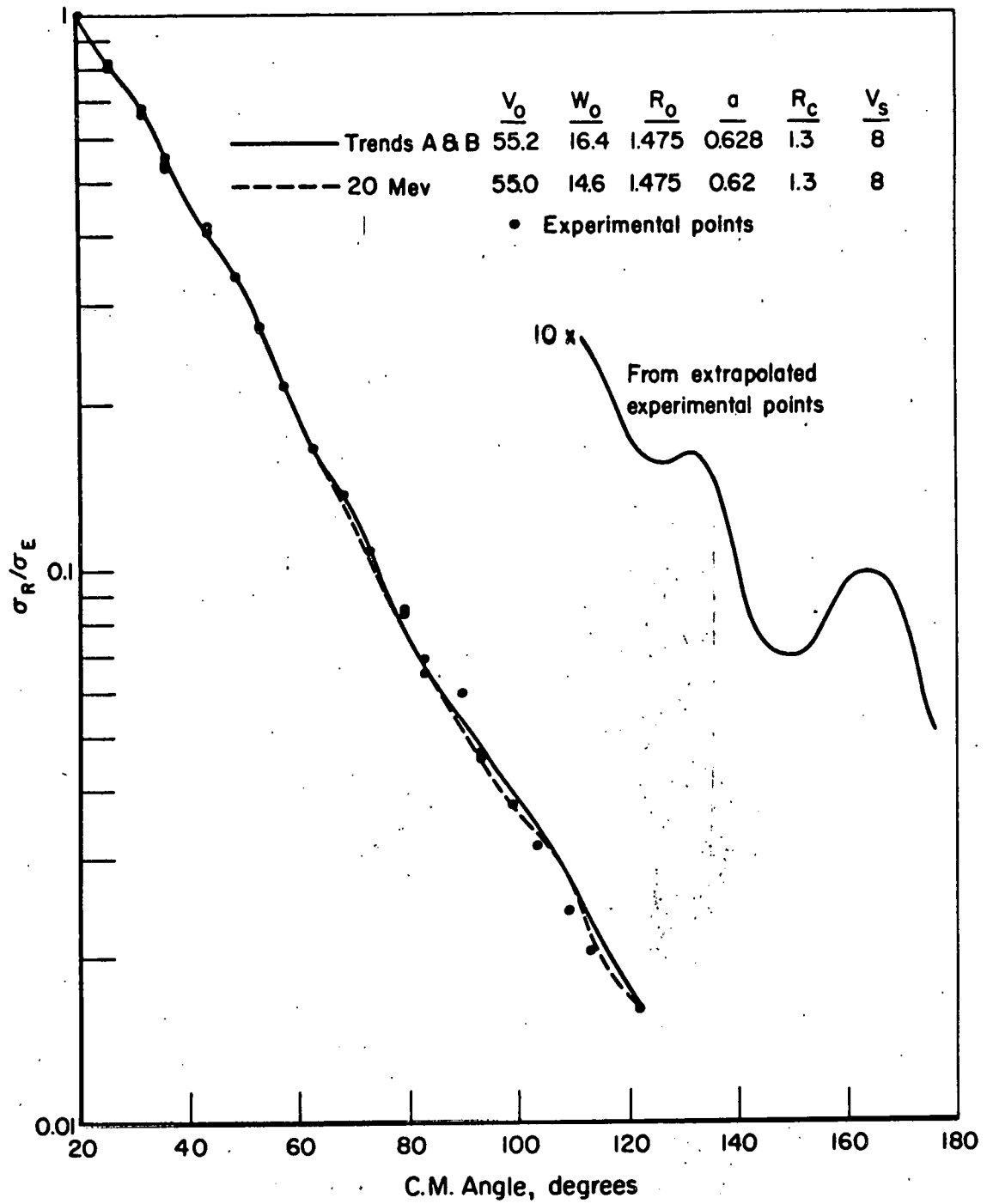
1
0.1
0.01
σ_R/σ_E
20
40
60
80
100
120
140
160
180
C.M. Angle, degrees
V_0 W_0 R_0 a R_c V_s
Trends A & B 55.2 16.4 1.475 0.628 1.3 8
20 Mev 55.0 14.6 1.475 0.62 1.3 8
• Experimental points
10 x
From extrapolated experimental points

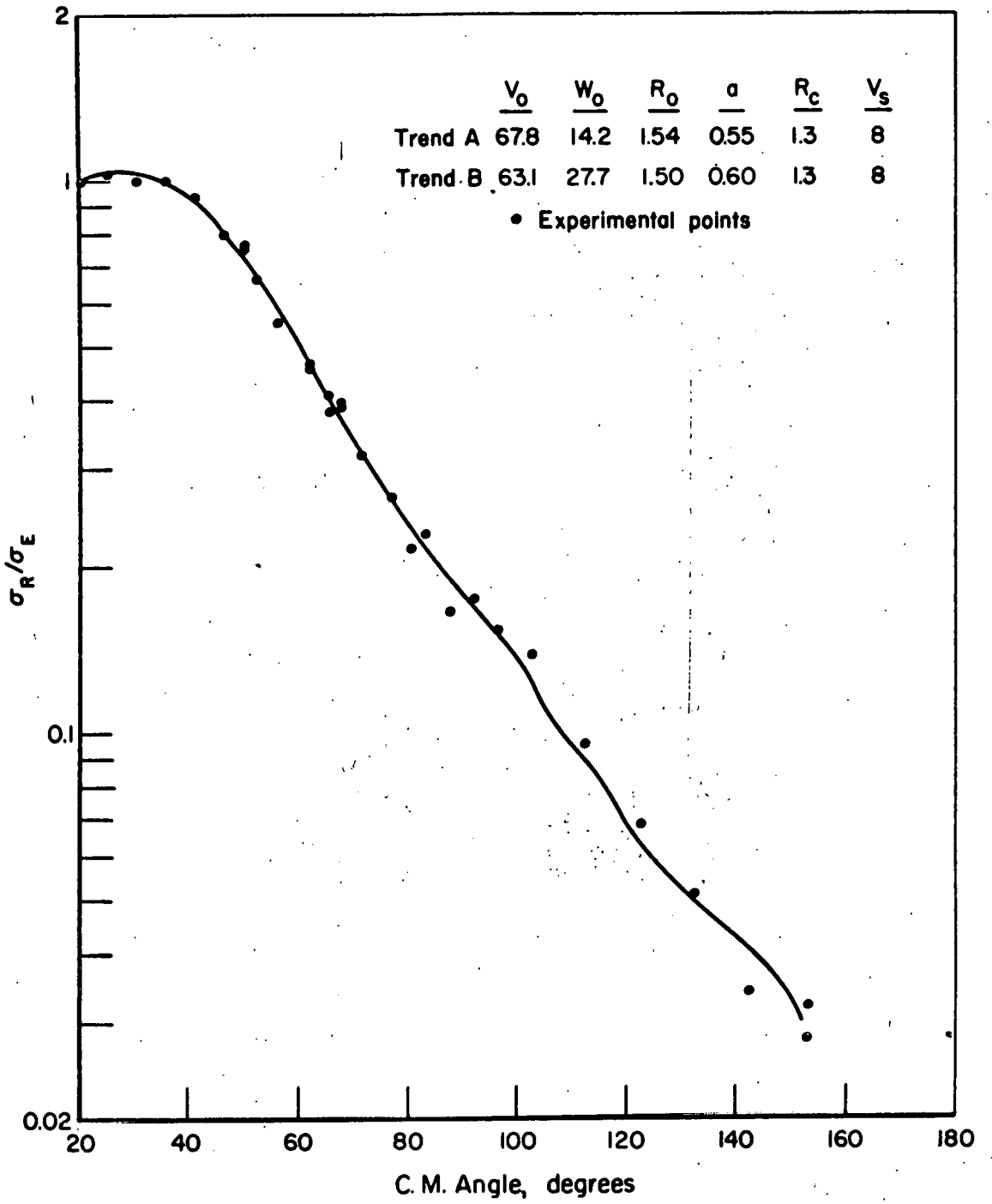
2
1
0.1
0.02
σ_R/σ_E
20
40
60
80
100
120
140
160
180
C. M. Angle, degrees
V_0 W_0 R_0 a R_c V_s
Trend A 67.8 14.2 1.54 0.55 1.3 8
Trend B 63.1 27.7 1.50 0.60 1.3 8
• Experimental points

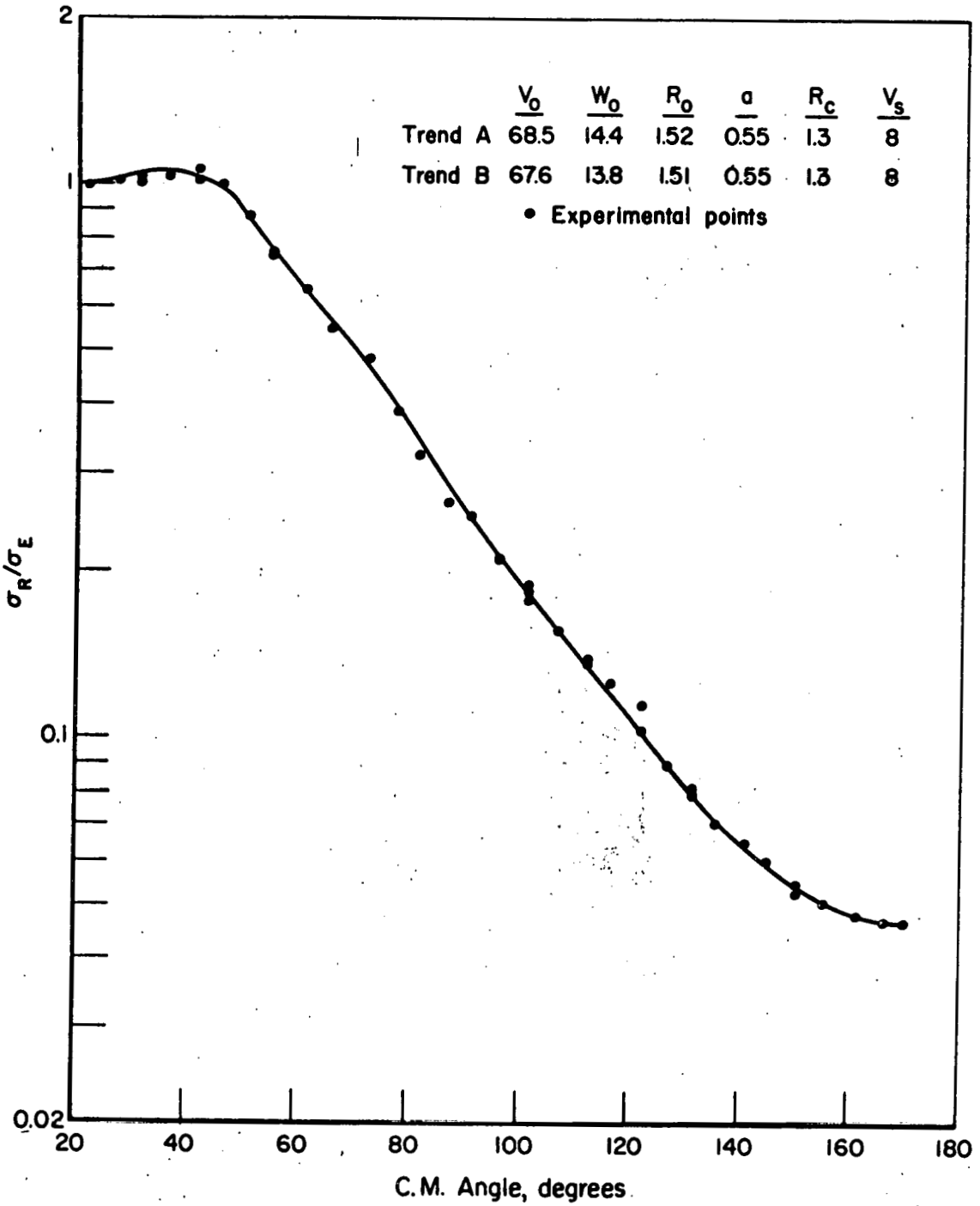
2
1
0.1
0.02
σ_R/σ_E
V_0 W_0 R_0 a R_c V_s
Trend A 68.5 14.4 1.52 0.55 1.3 8
Trend B 67.6 13.8 1.51 0.55 1.3 8
• Experimental points
20 40 60 80 100 120 140 160 180
C.M. Angle, degrees

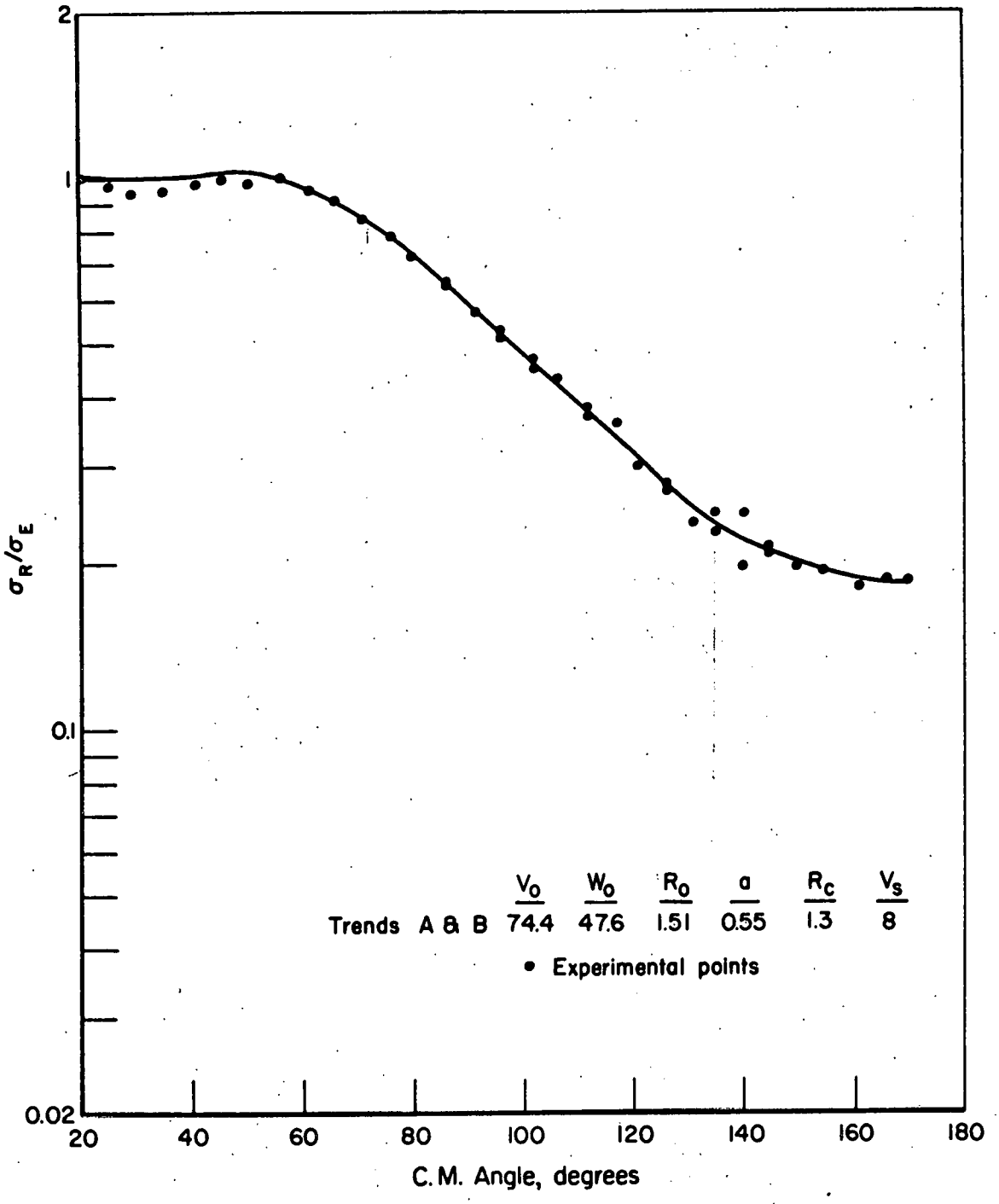
2
1
0.1
0.02
σ_R/σ_E
20
40
60
80
100
120
140
160
180
C.M. Angle, degrees
V_0 W_0 R_0 a R_c V_s
Trends A & B 74.4 47.6 1.51 0.55 1.3 8
• Experimental points

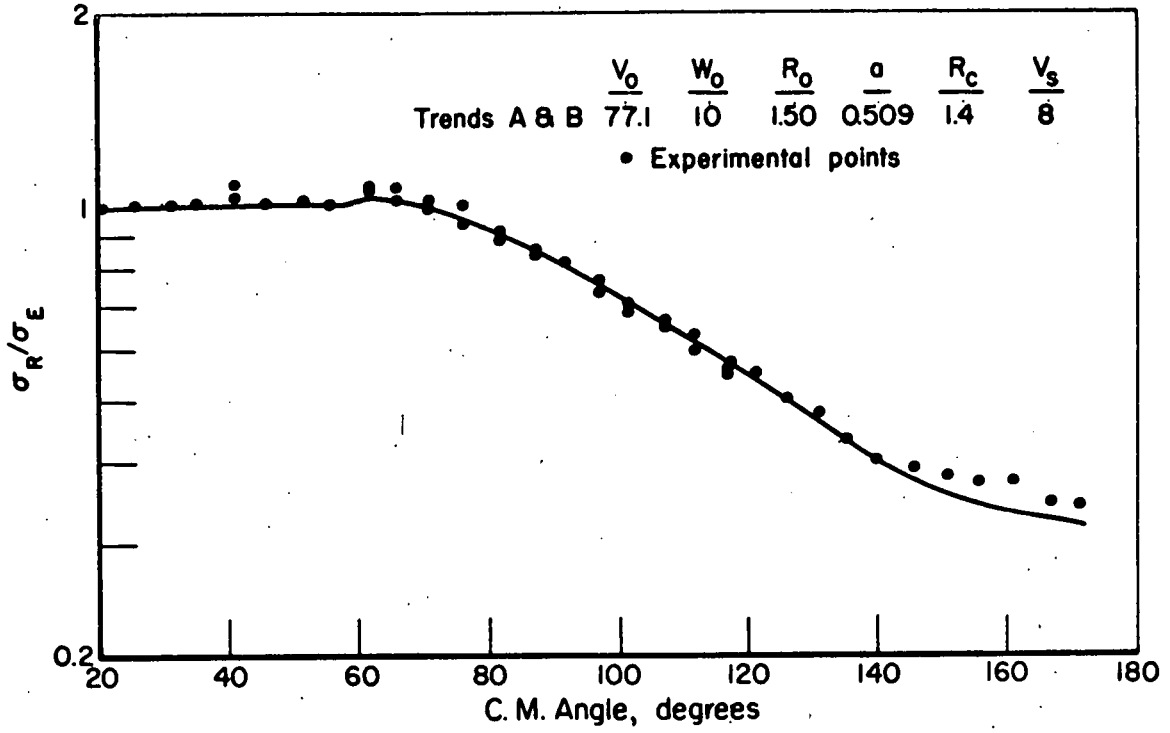
V_0 W_0 R_0 a R_c V_s
Trends A & B 77.1 10 1.50 0.509 1.4 8
• Experimental points
σ_R/σ_E
2
1
0.2
20 40 60 80 100 120 140 160 180
C. M. Angle, degrees

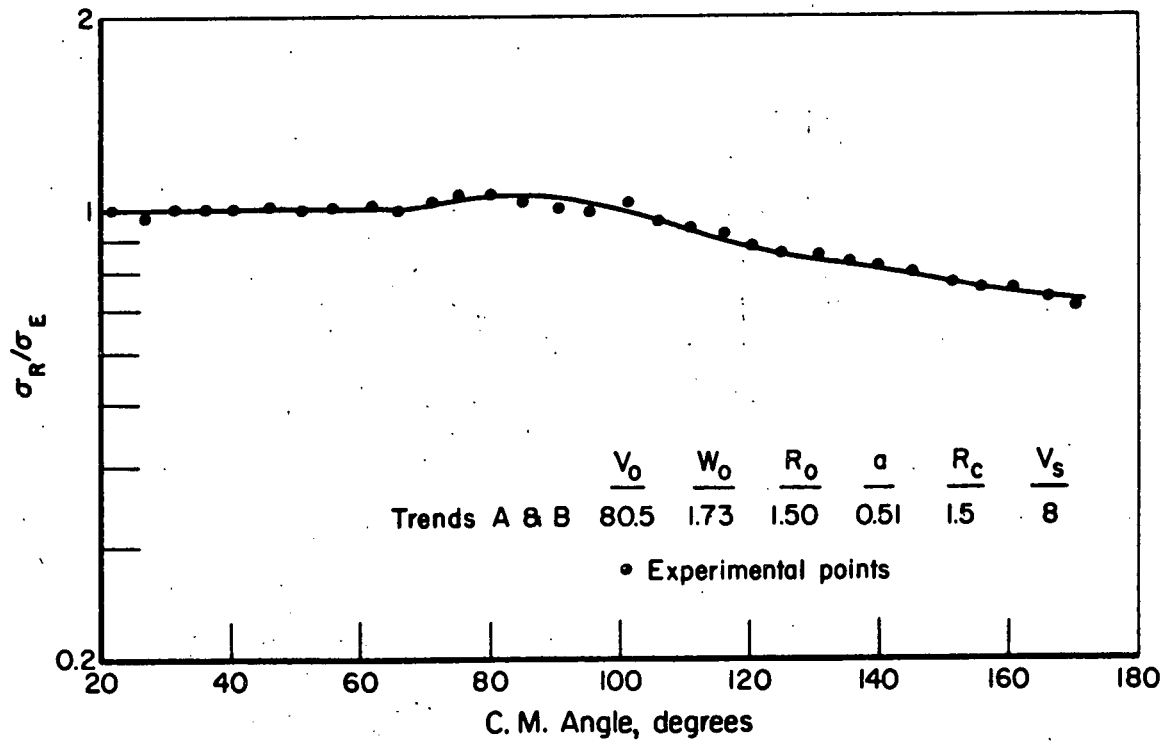
V_0 W_0 R_0 a R_c V_s
Trends A & B 80.5 1.73 1.50 0.51 1.5 8
• Experimental points
σ_R/σ_E
2
1
0.2
20 40 60 80 100 120 140 160 180
C. M. Angle, degrees